THE ASTROPHYSICAL JOURNAL, 510:651–658, 1999 January 10
© 1999. The American Astronomical Society. All rights reserved. Printed in U.S.A.

OBSERVATION OF CENTAURUS A BY THE *ROSSI X-RAY TIMING EXPLORER*

R. E. ROTHSCHILD, D. L. BAND, P. R. BLANCO, D. E. GRUBER, W. A. HEINDL, D. R. MACDONALD, AND D. C. MARSDEN
Center for Astrophysics and Space Sciences 0424, University of California at San Diego, La Jolla, CA 92093

K. JAHODA, D. PIERCE, AND G. MADEJSKI
NASA Goddard Space Flight Center, Greenbelt, MD 20771

M. ELVIS AND D. A. SCHWARTZ
Center for Astrophysics, Harvard-Smithsonian Astrophysical Observatory, Cambridge, MA 02138

R. REMILLARD
Center for Space Research, Massachusetts Institute of Technology, Cambridge, MA 02139

A. A. ZDZIARSKI
Nicolaus Copernicus Astronomical Center, Warsaw, Poland

C. DONE
Department of Physics, University of Durham, Durham, England

AND

R. SVENSSON
Stockholm Observatory, Saltsjöbaden, Sweden
Received 1998 May 11; accepted 1998 August 14

ABSTRACT

The *Rossi X-Ray Timing Explorer* made a short (10 ks) observation of the radio galaxy Centaurus A on 1996 August 14. Analysis of the combined 2.5–240 keV spectrum has revealed a heavily absorbed ($N_{\rm H} = 9.42 \pm 0.24 \times 10^{22}$ cm^{-2}) primary power law ($\Gamma = 1.86 \pm 0.015$) and an iron line due to fluorescence of cold matter (EW = 162 ± 25 eV). Flux from a jet, a primary flux scattered into the line of sight, or a primary flux seen through a partial absorber was not required. The iron-line width is unresolved at the 95% confidence level ($\sigma < 0.54$ keV). No significant variability in the iron-line flux is seen from measurements over the last two decades, while the overall continuum flux varied by more than a factor of 4, which implies that the line emission region is distant from that of the primary emission. While radio-quiet Seyfert galaxies exhibit spectral components attributable to Compton reflection from cold matter, Cen A reveals no such component (exposed solid angle ratio $\Omega/2\pi \leq 0.09$). This supports unified models of active galaxies that have little difference between Seyfert 2 and low-luminosity radio galaxies.

Subject headings: galaxies: active — galaxies: individual (Centaurus A) — galaxies: jets — galaxies: Seyfert — X-rays: galaxies

1. INTRODUCTION

Centaurus A (NGC 5128) was discovered in X-rays over 25 yr ago (Bowyer et al. 1970) and has been observed by most X-ray astronomy missions since then (see compilations in Baity et al. 1981 and Jourdain et al. 1993). At a distance of $\sim$3.5 Mpc (Hui et al. 1993), Cen A is one of the nearest active galactic nuclei (AGNs). Even though the nucleus is heavily obscured (in part by the famous dust lane that is seen to cross the galaxy), Cen A is one of the brightest extragalactic X-ray sources. Furthermore, Cen A is clearly a radio-loud object, displaying prominent radio jets and lobes (Burns, Feigelson, & Schreier 1983) and, as such, has provided much of our information on the high-energy nature of low-luminosity radio-loud AGNs. A comparison of Cen A with the well-studied Seyfert galaxies (Nandra & Pounds 1994; Nandra et al. 1997; Turner et al. 1997b, 1997c) as well as other radio-loud AGNs, in the context of the unified model for AGNs (e.g., Antonucci 1993; Woźniak et al. 1998), can yield insight into the differences between radio-loud and radio-quiet AGNs.

One area of radio-loud/radio-quiet difference is in the amount of the observed Compton "reflection" component. Compton reflection and line fluorescence (especially from iron) are important diagnostics of the central engine structure. Many Seyfert (i.e., radio-quiet) nuclei show these strong features, which are widely believed to result from irradiation of a thin accretion disk by a disk corona (Guilbert & Rees 1988; Lightman & White 1988; George & Fabian 1991). This component manifests itself as an iron line at 6.4 keV, an iron edge at 7.1 keV, and a hardening of the spectral slope above 10 keV, compared with the 2–10 keV spectrum. Many radio sources (including Cen A) appear to have significantly weaker reflection features than do Seyfert nuclei (Woźniak et al. 1998; Zdziarski et al. 1995; Grandi et al. 1997). Indeed, in most radio-loud objects there is no strong Compton reflection continuum, and the iron line is interpreted as originating in Thompson-thin circumnuclear material. In addition, for the case of Cen A the spectrum extends to 1 MeV (Steinle et al. 1998), while in radio-quiet Seyferts there is no indication of flux beyond a few hundred keV (Johnson et al. 1997). This, too, may indicate a difference in the flow of matter in the vicinity of the accretion disk, such as advection-dominated accretion flow versus thin disk accretion, and the presence of the collimated radio jet.

Previous observations have shown Cen A to have highly complex X-ray/gamma-ray properties (Döbereiner et al. 1996; Turner et al. 1997a; Feigelson et al. 1981) with multitemperature diffuse flux, a spatially resolved jet in radio and X-rays, and a nuclear component with complex low-energy absorption. The observed iron line at 6.4 keV of equivalent width $\sim$100 eV is consistent with reprocessing from the

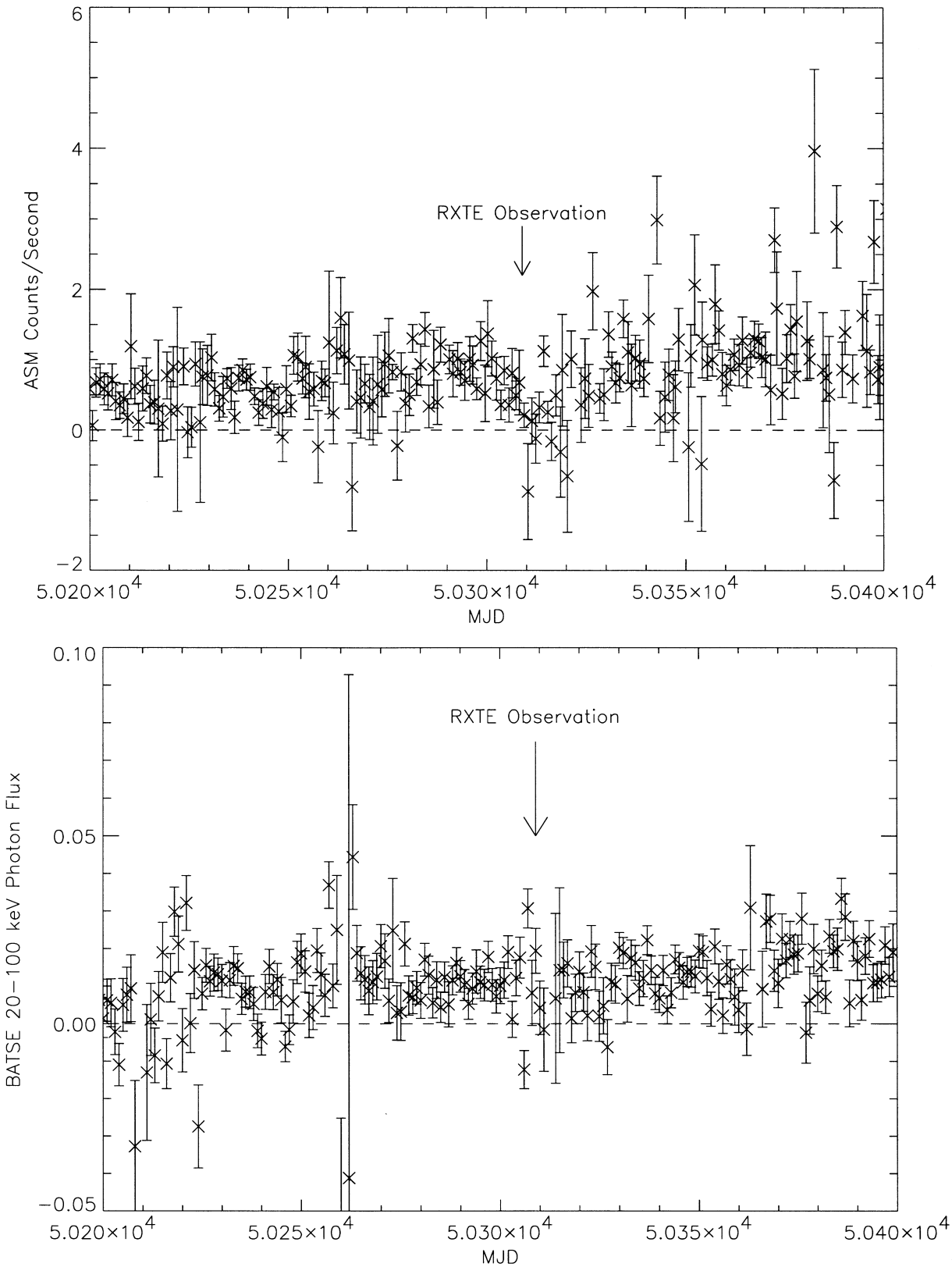

FIG. 1.—*RXTE* ASM daily average counting rates in the 2–12 keV band and the *CGRO*/BATSE Earth-occultation fluxes in the 20–100 keV band for Cen A during 200 days centered on the *RXTE* pointed observation. The arrow indicates the date of the Cen A observation.

absorbing material (Turner et al. 1997a; Sugizaki et al. 1997). At energies above ~ 10 keV, Woźniak et al. (1998) analyzed *Ginga* data and found no evidence for a strong Compton reflection component ($\Omega/2\pi < 0.15$) in addition to the heavily absorbed ($N_{\rm H} = 1.7 \pm 0.1 \times 10^{23}$ cm^{-2}) power law ($\Gamma = 1.79^{+0.06}_{-0.05}$). This implies that there is little cold, Thompson-thick material in the close vicinity of the AGN (Woźniak et al. 1998) that reflects X-rays into our line of sight. Taken together with the iron-line equivalent width, this result is consistent with transmission of the primary

flux through the line-of-sight absorber and viewing the accretion disk nearly edge-on. *Compton Gamma Ray Observatory* (*CGRO*)/OSSE observations reveal a steepening of the spectrum at 140–170 keV, which might be due to a nonthermal electron distribution in the central engine (Kinzer et al. 1995). The *CGRO*/COMPTEL and *CGRO*/EGRET instruments indicate that this steepening trend continues to 1 GeV with spectral indices ranging from 2.6 to 3.3 depending on intensity (Steinle et al. 1998).

In this paper we present the results of a short, 10 ks observation of Cen A by the *Rossi X-Ray Timing Explorer* (*RXTE*) in the range 2.5–240 keV. Section 2 details the observations, § 3 presents the data reduction and analysis, § 4 discusses the results with respect to Cen A itself and in the larger view of AGN unification, and § 5 presents the conclusions.

2. OBSERVATIONS

The *RXTE* observed Cen A from 2:43 to 8:05 UT on 1996 August 14 with the Proportional Counter Array (PCA) and the High Energy X-Ray Timing Experiment (HEXTE). The PCA contains five large-area, xenon, multiwire, multilayer, gas proportional counter units that cover the energy range 2–60 keV with energy resolution of 1 keV at 6 keV (Jahoda et al. 1996). All five proportional counters were used in this observation, for a total open area of ~ 7000 cm^2. The field of view of each PCA unit is constrained to 1° FWHM by a beryllium/copper honeycomb collimator, and all five are co-aligned to within 5′ to the spacecraft science pointing axis.

The HEXTE consists of two independent clusters of detectors, each cluster containing four NaI(Tl)/CsI(Na) phoswich scintillation counters, each identically collimated by a lead honeycomb (Rothschild et al. 1998). All eight collimators are co-aligned with the PCA on source to give both clusters a 1° FWHM field of view. The net open area of the eight detectors is ~ 1600 cm^2, and each detector covers the energy range 15–250 keV with an average energy resolution of 9 keV at 60 keV.

Throughout the *RXTE* mission, the All-Sky Monitor (ASM) provides an estimate of the 1.5–12 keV flux from the 100 brightest X-ray sources on a 90 minute and daily basis. The ASM is composed of three scanning shadow cameras, each of which is a position-sensitive xenon proportional counter that views a $6° \times 90°$ FWHM section of sky through a one-dimensional coded mask (Levine et al. 1996). Each camera has ~ 30 cm^2 at 5 keV.

Figure 1 shows the *RXTE* ASM counting rate for Cen A in the 1.5–12 keV range for 200 days, centered on the *RXTE* pointed observation. The day of the observation (MJD 50,309) is indicated in the figure and is at or shortly after the beginning of an interval of lower than average flux. Comparison of PCA and ASM fluxes indicates that the PCA/HEXTE observations were made at or near the lower flux level. The four PCA/HEXTE viewing intervals, separated by Earth occults and South Atlantic Anomaly (SAA) passages, do not reveal any significant change in intensity over the 5.5 hr of the observation. Also shown are the 20–100 keV fluxes measured on a daily average by *CGRO*/BATSE using the Earth occultation technique. The BATSE data are not sensitive to the magnitude of temporal variation seen by the ASM, as is evidenced by the BATSE error bars. Thus, the *RXTE* observation appears to have occurred during a temporary period of lower intensity than for the few weeks on either side of the observation. While this rate is low vis-à-vis the weeks surrounding the observation, it is quite typical when compared with past observations.

3. DATA REDUCTION AND ANALYSIS

The PCA standard data were used for the accumulation of spectra and light curves, while the HEXTE standard data provided the HEXTE spectral histograms and light curves. The data from both instruments were accumulated on 16 s intervals, and no significant variability was noted. The PCA response matrix used was dated 1998 April 24. Estimates of systematic errors were added to the statistical errors for the PCA spectral data in order to reduce the effects of imperfect knowledge of the instrument response near the K and L edges of xenon. These errors were 0.5% from 2.5 to 5.5 keV, 1% from 5.5 to 8 keV, 0.5% from 8 to 20 keV, and 3% from 20 to 90 keV. These values were determined from residuals to fits to the Crab Nebula observations. No additional systematic errors were incorporated in the HEXTE data, because the statistical errors were larger than the few percent systematic errors reported in Rothschild et al. (1998).

3.1. *Background Subtraction*

The PCA background was estimated using models of the instrument background, activation, and the cosmic diffuse flux derived from blank sky observations obtained throughout 1997. We were able to provide a good background estimate over the entire PCA range by selecting non-SAA and nonocculted data and removing time intervals of electron precipitation as evidenced by raw rates in various layers of the PCA. The PCA analysis was performed over the 2.5–60 keV range. PCA source and background rates in various energy channels are given in Table 1.

Contrary to lower energy measurements, hard X-ray observations are made in a background-dominated regime, except for the brightest sources. The background, therefore, must be measured during each observation on timescales that are short compared with those for background variations. Modeling background from counting rates is at least an order of magnitude less accurate and is not appropriate for hard X-ray measurements. The HEXTE cluster-rocking

TABLE 1

PCA AND HEXTE COUNTING RATES

Range Analyzed (keV)	Cen A (counts s^{-1})	Background (counts s^{-1})	Cen A/Background
PCA (5 Detectors)			
2–10	100.5 ± 0.25	31.45 ± 0.05	3.20 ± 0.008
10–20	37.71 ± 0.11	25.27 ± 0.05	1.49 ± 0.004
20–60	7.25 ± 0.35	67.57 ± 0.08	0.11 ± 0.005
HEXTE A (4 Detectors)			
15–30	2.99 ± 0.13	24.57 ± 0.10	0.122 ± 0.005
30–100	2.38 ± 0.24	80.23 ± 0.18	0.030 ± 0.003
100–240	0.24 ± 0.20	54.88 ± 0.15	0.004 ± 0.004
HEXTE B (3 Detectors)			
15–30	2.21 ± 0.11	15.76 ± 0.08	0.140 ± 0.007
30-100	1.98 ± 0.21	60.14 ± 0.16	0.033 ± 0.003
100–240	0.04 ± 0.17	38.86 ± 0.13	0.001 ± 0.004

subsystem moves the viewing direction of the detector arrays in a cluster between on-source and off-source every 16 s in order to obtain the near–real-time measurement of the instrument background. The nominal angular offset of 1°.5 on either side of the on-source position was used in the Cen A observation. Since the rocking axes of the two clusters are orthogonal to each other, four background regions were sampled around Cen A's position. No confusing sources were detected. This technique provides background subtractions that are not based on any modeling and are direct measurements taken during each observation. Analysis of blank fields demonstrated that the net blank-field flux was consistent with zero, with residuals of 1% of background or less (Rothschild et al. 1998). The HEXTE analysis was performed over the 15–240 keV range. HEXTE source and background rates in various energy channels are given in Table 1.

3.2. *Spectrum*

The PCA and HEXTE data were fitted simultaneously using the XSPEC 10.0 package with the relative normalization of the two instruments included as a fitted parameter. We utilized a model that contained a heavily absorbed power law plus Gaussian emission line to represent the primary flux. The best-fit values for the case of the emission-line width set to zero are given in Table 2. All error bars, unless specified differently, are 95% confidence and are generated by varying one parameter and fitting all others. The decrease in χ^2 that occurred when the line width was included as a free parameter was 5.2 for one additional degree of freedom out of 540. The F-test indicates that the probability of this being a fluctuation is 0.021 and therefore is not significant at the 98% level. The range of the iron-line width at the 95% confidence level is 0.11 keV $< \sigma$ (FWHM) < 0.54 keV. The energy of the line, 6.46 ± 0.097 keV, indicates that the emission is from cool, i.e., weakly ionized, material. The best-fit model with a narrow line is shown in Figure 2 as the predicted instrument counts histogram compared with the observed counts histogram. This figure has not been corrected for the relative normalization of the two HEXTE clusters with respect to the PCA (see Table 2). The inferred incident spectrum is shown in Figure 3 in the form of νF_ν versus energy with the HEXTE flux normalized to the PCA and with the points from both detector systems rebinned for display purposes. The data from the two HEXTE clusters have also been combined into a single spectrum.

Turner et al. (1997a) reported an additional component from *ROSAT* observations of the jet from Cen A, which is characterized by a power law with photon index $\Gamma = 2.29^{+0.67}_{-0.46}$ or a thermal bremsstrahlung model with $kT = 1.27^{+1.21}_{-0.44}$. We tested the Cen A spectrum for the presence of an additional unabsorbed component in two ways. The first was by the addition of a power law whose photon index was a free parameter in the fitting. The decrease in χ^2 was 4.0 for two additional parameters. The F-test indicates a probability of 0.13 that a fluctuation could have produced such a value. The second test was to utilize a partial covering fraction model of the absorber that would allow for a percentage of the primary flux to be transmitted through the absorber. In this case the χ^2 decreased by 7.4, which, again, is less than a 3 σ improvement. The 95% confidence range is 1.3%–6.6% for the fraction of the primary flux that is transmitted. As a result, we conclude that an additional unabsorbed component was not required by the short *RXTE* observation.

The *RXTE* data were tested for the presence of a spectral break or steepening at higher energies using a broken power law. The best-fit broken power-law model was consistent with no break at all, and the power-law index above the break energy (held fixed at 140 keV) was essentially unconstrained. This result is due to the small number of counts in HEXTE above 100 keV in this short observation. This is consistent with the *CGRO*/OSSE (Kinzer et al. 1995) and *Welcome-1* (Miyazaki et al. 1996) results that extend to higher energies.

In order to test for the presence of a Compton reflection component, two fits were made to the data. First, an absorption edge at 7.1 keV was added to the heavily absorbed primary power law. This resulted in an upper limit to the absorption depth of $\tau \leq 0.016$, indicating that no strong reflection component was present. The lack of an iron absorption edge in the data also implies that improper modeling of the continuum does not affect the inferred width of the fitted Fe line (see Zdziarski, Johnson, & Magdziarz 1996 for a discussion of this systematic effect in NGC 4151). This was further confirmed by substituting a power law plus Compton component (XSPEC 10.0 model PEXRAV; Magdziarz & Zdziarski 1995) for the primary power law in the model. The 90% upper limit to a reflection

TABLE 2

FIT TO PCA (2.5–60 keV)/HEXTE (15–240 keV) SPECTRA

Best-Fit Spectrum	
Absorption	$N_H = 9.42 \pm 0.24 \times 10^{22}$ cm^{-2}
Power law	$\Gamma = 1.857 \pm 0.015$
	F(2–10 keV) $= 3.398 \pm 0.052 \times 10^{-10}$ ergs cm^{-2} s^{-1}
Iron line	$E_{Fe} = 6.46 \pm 0.097$ keV
	σ (FWHM) $= 0$
	F(6.46 keV) $= 5.37 \pm 0.83 \times 10^{-4}$ photons cm^{-2} s^{-1}
	EW $= 162 \pm 25$ eV
Normalization.....	Cluster A[a] $= 0.688 \pm 0.020$
	Cluster B[b] $= 0.693 \pm 0.024$
	Flux(2–10 keV) $= 1.972 \pm 0.002 \times 10^{-1}$ ergs cm^{-2} s^{-1}
Fit	χ^2/dof $= 517.2/541$
	$\chi^2_\nu = 0.956$

[a] Ratio of HEXTE to PCA normalization for cluster A.
[b] Ratio of HEXTE to PCA normalization for cluster B.

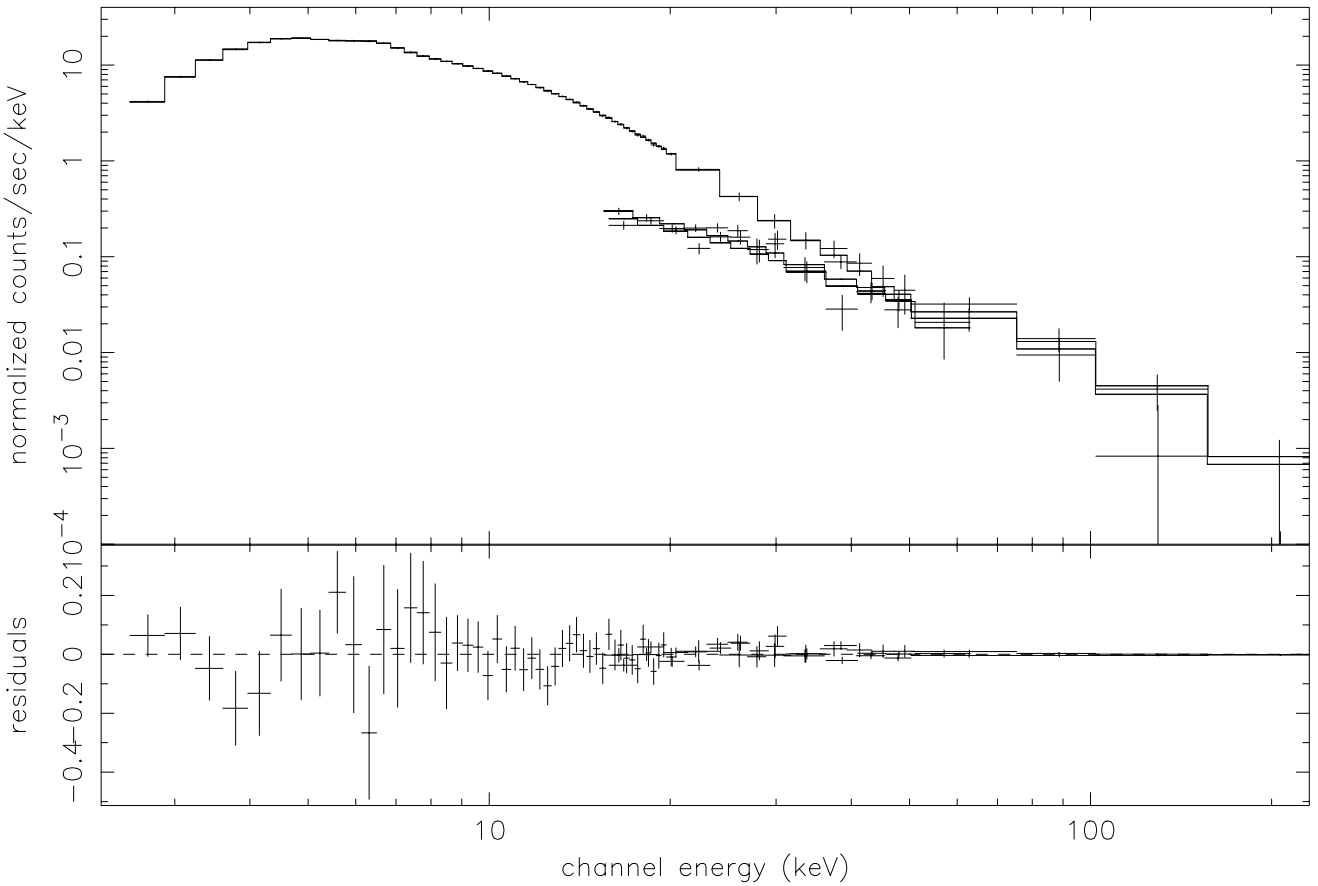

FIG. 2.—PCA and HEXTE spectral histograms plus best-fit model for the *RXTE* observation of Cen A. The lower panel shows the residuals to the fit. The relative normalization of each HEXTE cluster has been left as a free parameter in the fitting process. The difference between the two HEXTE sets of data are the result of having data from only three of the four detectors in cluster B. The HEXTE high-energy data has been rebinned for display purposes.

TABLE 3

PREVIOUS OBSERVATIONS OF THE IRON LINE IN CEN A

Satellite	Observation Date	Photon Index	Absorption[a]	Equivalent Width[b]	Line Flux[c]	Source Flux[d]	Reference
OSO-8	1975 Jul 27–Aug 5	1.66 ± 0.03[e]	1.33 ± 0.07[e]	120 ± 35[e]	5.7 ± 1.7[f]	4.66 ± 0.06	1
OSO-8	1976 Jul 28–Aug 8	1.66 ± 0.03[e]	1.33 ± 0.07[e]	120 ± 35[e]	5.7 ± 1.7[f]	2.39 ± 0.11	1
EXOSAT.....	1984 Feb 13	1.75 ± 0.08	1.64 ± 0.08	164 ± 36	4.7 ± 1.0	3.4 ± 0.5	2
Tenma	1984 Mar 29–Apr 4	1.80 ± 0.04	1.53 ± 0.03	90 ± 20	5.5 ± 1.2[f]	7.6 ± 0.07	3
EXOSAT.....	1984 Jun 8	1.57 ± 0.10	1.40 ± 0.10	207 ± 52	3.7 ± 0.9	2.6 ± 0.5	2
EXOSAT.....	1984 Jul 30	1.61 ± 0.08	1.70 ± 0.09	145 ± 43	3.1 ± 0.9	2.9 ± 0.4	2
EXOSAT.....	1985 Jun 29	1.70 ± 0.02	1.44 ± 0.02	63 ± 9	5.7 ± 0.8	11.3 ± 0.3	2
Ginga	1989 Mar 8–9	1.80 ± 0.02	$1.61^{+0.07}_{-0.05}$	110 ± 32	$5.2^{+0.9}_{-1.0}$	2.3 ± 0.1	4
Ginga	1990 Feb 7–9	1.81 ± 0.02	1.43 ± 0.03	110 ± 32	5.2 ± 0.9	2.3 ± 0.1	4
ASCA.....	1993 Aug 14	$1.83^{+0.5}_{-0.4}$	1.29 ± 0.40	68 ± 39	3.07 ± 1.72[f]	1.78 ± 0.18	5
ASCA.....	1993 Aug 14–15	1.96 ± 0.01	$1.10^{+0.02}_{-0.01}$ (59%)	114 ± 18	$3.91^{+0.46}_{-0.47}$	1.8 ± 0.06	6
	...	...	$3.54^{+0.20}_{-0.24}$ (40%)	...	...	...	
RXTE	1996 Aug 14	1.86 ± 0.015	0.94 ± 0.02	162 ± 25	5.37 ± 0.83	3.40 ± 0.05	7

[a] $\times 10^{23}$ cm^{-2}.
[b] Equivalent width in eV.
[c] $\times 10^{-4}$ photons cm^{-2} s^{-1}.
[d] $\times 10^{-10}$ ergs cm^{-2} s^{-1} in the 2–10 keV band.
[e] Average of the 1975 and 1976 data.
[f] Calculated from parameters given in reference.

REFERENCES.—(1) Mushotzky et al. 1978; (2) Morini, Anselmo, & Molteni 1989; (3) Wang et al. 1986; (4) Miyazaki et al. 1996; (5) Sugizaki et al. 1997; (6) Turner et al. 1997a; (7) present work.

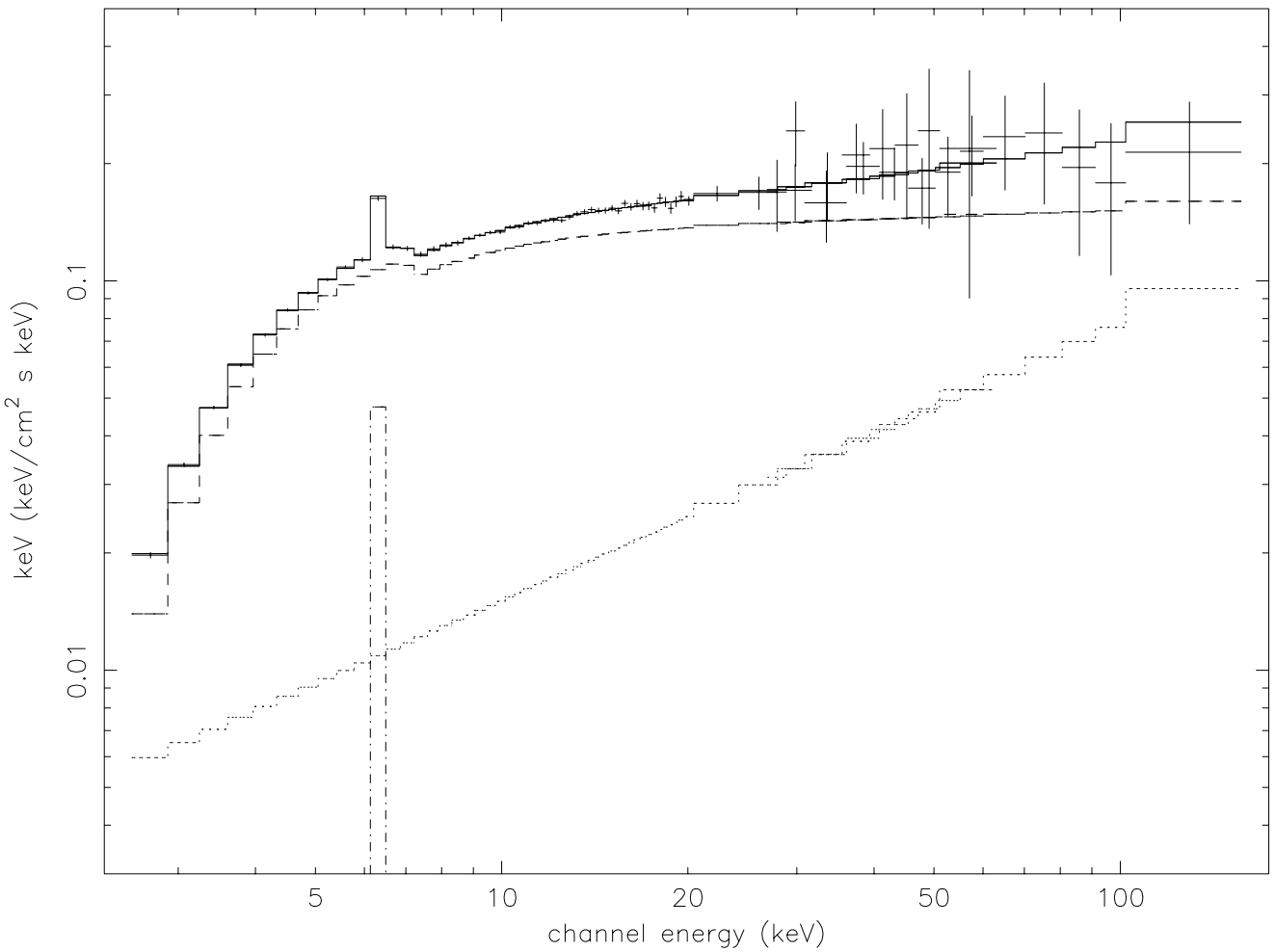

FIG. 3.—Energy flux vs. energy for the best-fit power-law model containing a heavily absorbed power law and a broad iron line, plus a nonabsorbed power law. The HEXTE data have been combined into a single spectrum and normalized to the PCA flux. Both PCA and HEXTE data have been rebinned for display purposes.

component, expressed as the ratio of the solid angle for primary flux scattered into our line of sight to an infinite slab, was found to be $\Omega/2\pi \leq 0.088$ for an assumed inclination angle of 70°.

When we modeled the iron line as coming from a relativistic accretion disk with an r^{-2} dependence of the emissivity from 10 to 1000 GM counts^{-2}, we found the disk inclination to not be constrained by the observations (90% confidence interval includes all angles from 0° to 90°), and the resulting centroid was consistent with the Gaussian line fits. The other model parameters are not substantially changed, and the $\Delta\chi^2 = 5.0$ with respect to the narrow line model was not significant (probability = 0.024). Thus, two indications of observed X-ray emission from an accretion disk—a Compton reflection spectrum and an iron line from a disk—are not required by the present data.

To recapitulate, the *RXTE* spectrum of Cen A can be best described by a heavily absorbed power law extending above 100 keV and a 162 ± 24 eV equivalent width iron line from cold matter. The FWHM of the iron line is less than 0.54 keV and is therefore taken to be narrow. Measurement of a steepening in the power law above 100 keV is precluded by the small number of counts in that range for this short observation. Neither an additional unabsorbed low-energy component nor a Compton reflection component are required to fit the data.

The *RXTE* best fit can be compared with the *ASCA* (Sugizaki et al. 1997; Turner et al. 1997a) and *Ginga* (Woźniak et al. 1998) results. The *RXTE* power-law index of 1.857 ± 0.008 agrees with the *ASCA* and *Ginga* values. The measured absorption, however, has decreased about 60% from $\sim 1.6 \times 10^{23}$ cm^{-2} to the *RXTE* value of $0.94 \pm 0.01 \times 10^{23}$ cm^{-2} in 3 yr. At the same time the equivalent width of the narrow iron line has increased 33% from ~ 120 to ~ 160 eV. The flux of the Fe line, on the other hand, has not changed significantly (see Table 3). The *RXTE* and *Ginga* upper limits on the reflection component are in complete agreement, i.e., none is detected to less than $\Omega/2\pi \sim 0.09$. This can be compared with a weighted mean of 0.72 ± 0.05 for 27 *Ginga* Seyfert galaxies (Nandra & Pounds 1994). The latter sample was dominated by radio-quiet objects, with only three 3C sources included.

4. DISCUSSION

Observations of molecular lines in emission and absorption from Cen A (Israel et al. 1990) imply that a thick torus with outer radius of 325 pc, inner radius of 80 pc, and thickness of 80 pc surrounds the nucleus. The density of the

torus decreases as r^{-2} from an inner edge value of 2×10^4 cm^{-3}. With an estimated mass of $2 \times 10^7 M_\odot$, the line of sight through the torus would have $\sim 1.0 \times 10^{23}$ atoms cm^{-2}, which is consistent with past and present measurements in the X-ray range. Leahy & Creighton (1993) have simulated X-ray spectra for power-law fluxes embedded in a spherical absorber, and Figure 1 of Turner et al. (1997b) displays the result for a power-law photon index of 2. This calculation predicts about 100 eV equivalent width for a column density of $\sim 1 \times 10^{23}$ cm^{-2}. If the iron line were due to reprocessing of the primary flux in a cold accretion disk by Compton reflection, on the other hand, equivalent widths close to 300 eV would be expected. The present Cen A result of 162 ± 24 eV equivalent width and no evidence of a Compton component is consistent with the iron emission coming from a power-law flux embedded in a uniform spherical absorber.

Over the last two decades, the flux from the iron line and the continuum flux have been measured by instruments on *OSO-8*, *EXOSAT*, *Tenma*, *Ginga*, *ASCA*, and now *RXTE*. Table 3 gives the published history of these measurements of the spectral index, absorbing column, iron-line equivalent width, iron-line flux, and 2–10 keV flux from Cen A. The multiple observations by *OSO-8* and *EXOSAT* each claim no variation in iron-line flux while reporting changes in 2–10 keV continuum flux of factors of 2 or more. On the other hand, both the line and continuum fluxes are reported to be essentially constant for the two *Ginga* observations. Over the last 20 yr the absorbing column depth has ranged over $1\text{–}2 \times 10^{23}$ cm^{-2}, while the equivalent width has values from less than 50 to greater than 200 eV. Comparison with the Leahy & Creighton (1993) model displayed in Figure 1 of Turner et al. (1997b) shows that the equivalent width/absorbing column values scatter about the calculation for circumnuclear material with, at most, factor of 2 deviations above and below the model predictions.

Does the iron-line flux vary? Fitting the data in Table 3 to a single mean value of 4.65×10^{-4} photons cm^{-2} s^{-1} yields a $\chi_\nu^2 = 1.15$ for 10 degrees of freedom. This implies that the line fluxes are consistant with a single value. At the same time, the mean continuum flux is 3.86×10^{-10} ergs cm^{-2} s^{-1}, with a large scatter about this value. Fitting to this mean value yields a χ_ν^2 in the thousands. Clearly the iron line originates far away from the nucleus. Because of the sparse sampling of Cen A by instruments capable of measuring the iron line and continuum flux, one cannot test for time delays between continuum variations and those in the line flux, which might support the molecular torus as the site of the iron-line emission.

Using *ASCA* data, Sugizaki et al. (1997) found a hard nuclear and a soft diffuse component plus low-Z lines of Mg, Si, and S and the high-Z line from Fe. The soft component had a factor of 10 less absorbing column depth than the hard component, indicating that it was not being viewed through the torus. The equivalent widths of the low-Z lines and the soft continuum were compatible with being produced by the primary hard flux scattered by cold matter. The iron-line equivalent width, under the same assumptions, was a factor of 2 larger than expected. From this, Sugizaki et al. (1997) concluded that the low-Z–emitting material and the material responsible for the Fe line must be located in separate regions. This further implies that the covering factor of the primary source must be less than unity for the primary flux to reach the reprocessing site. This is consistent with the unified model, where the molecular torus does not cover the poles but does impact observations of the primary flux from high inclination angles.

Nandra et al. (1997) have studied 18 Seyfert 1 galaxies with *ASCA* and find an average spectral behavior, using the relativistic disk model, that is compatible with unification models, i.e., photon indices averaging 1.9, equivalent widths of iron lines averaging 230 eV, and small ($\sim 30°$) inclination angles. The line widths are explained by emission from a range of radii in the accretion disk around a supermassive black hole, and emission from another region is not required. Importantly, another component to the iron emission due to observing the primary flux through a dense ($N_{\rm H} \approx 10^{23}$ atoms cm^{-2}) uniform medium is not required. Nandra & Pounds (1994) used the broadband *Ginga* observations of 20 Seyfert 1 and seven narrow emission line galaxies that are also classified as Seyfert 2 galaxies (Turner et al. 1997b) to investigate reflection components under the assumption of a face-on geometry. Reflection components were detected in roughly half of the samples of both types of Seyfert galaxies.

Turner et al. (1997b, 1997c) have summarized *ASCA* observations of 25 Seyfert 2 galaxies and thoroughly discussed the consequences of observing scattered and reflected X-rays. Several radio-quiet galaxies in their sample exhibited iron lines (EW > 200 eV) from cold ($E_{\rm Fe} = 6.4$ keV) material yet had little or no evidence for Compton reflection components, which is consistent with viewing the accretion disk at a high inclination angle. When combined with the Seyfert 1 observations, this indicates that the inner regions of near edge-on radio galaxies and radio-quiet Seyfert 2 galaxies are similar and that the unified model of active galaxies may be applicable independent of radio character. This further implies that the presence of the highly collimated jet in radio galaxies like Cen A plays a small part in determining the disk/reflection emission from active galaxies. On the other hand, when one is viewing within the collimated beam, as is the case for blazars, the jet dominates the X-ray and gamma-ray emission observed.

5. CONCLUSIONS

A short *RXTE* observation of Cen A during a short period of reduced flux has revealed no temporal variability over 5.5 hr and a complex spectrum in the 2–250 keV range. The best-fit spectral model consists of a heavily absorbed primary flux and an emission line from cool iron. The measured column depth, iron-line equivalent width, and power-law index are consistent with earlier observations. The iron-line flux has not been observed to vary in sparce sampling of it over the last two decades, while the continuum flux has varied dramatically, indicating that the iron-line emission occurs far from the primary X-ray emission site.

The line equivalent width is consistent with production in the molecular torus by the primary hard X-ray flux, and the weakness or lack of a Compton reprocessing component is consistent with the nearly edge-on view of the accretion disk. In addition, the lack of a line at 6.7 keV and no Compton component indicates that an ionized gas enveloping the broad line region is not scattering a significant amount of X-ray flux into our line of sight. Cen A's X-ray character is essentially the same as that of radio-quiet Seyfert 2 galaxies. This indicates that the presence of the collimated radio jet does not significantly affect the parameters of the matter within the inner parsec of the system and

that the unification model for radio-quiet AGNs may be extended to include low-luminosity radio galaxies. Future observations of Cen A will be made in 1998 and will be the basis for variability studies that may shed more light on the geometry of the inner region of this active galaxy.

We acknowledge the excellent work of the *RXTE* Science Operations Center staff to provide the observations and the Guest Observer Facility for providing support in analyzing them. We also thank A. Harmon and the BATSE instrument team for providing the BATSE data on Cen A and the thoughtful comments from the referee. This work was supported by NASA contract NAS 5-30720.

REFERENCES

Antonucci, R. 1993, ARA&A, 31, 473
Baity, W. A., et al. 1981, ApJ, 244, 429
Bowyer, C. S., Lampton, M., Mack, J., & de Mendonca, F. 1970, ApJ, 161, L1
Burns, J. O., Feigelson, E. D., & Schreier, E. J. 1983, ApJ, 273, L28
Döbereiner, S., et al. 1996, ApJ, 470, L15
Feigelson, E. D., Schreier, E. J., Delvaille, J. P., Giacconi, R., Grindlay, J. E., & Lightman, A. P. 1981, ApJ, 251, 31
George, I. M., & Fabian, A. C. 1991, MNRAS, 249, 352
Grandi, P., Sambruna, R. M., Maraschi, L., Matt, G., Urry, C. M., & Mushotzky, R. F. 1997, ApJ, 487, 636
Guilbert, P. W., & Rees, M. J. 1988, MNRAS, 233, 475
Hui, X., Ford, H. C., Freeman, K. C., & Dopita, M. A. 1993, ApJ, 414, 463
Israel, F. P., van Dishoeck, E. F., Baas, F., Koornneef, J., Black, J. H., & de Graauw, T. 1990, A&A, 227, 342
Jahoda, K., Swank, J. H., Giles, A. B., Stark, M. J., Strohmayer, T., Zhang, W., & Morgan, E. 1996, Proc. SPIE, 2808, 59
Johnson W. N., Zdziarski, A. A., Madejski, G. M., Paciesas, W. S., Steinle, H., & Lin, Y.-C. 1997, Proc. Fourth Compton Symposium, ed. C. D. Dermer, M. S. Strickland, & J. D. Kurfess (Woodbury: AIP), 283
Jourdain, E., et al. 1993, ApJ, 412, 586
Kinzer, R. L., et al. 1995, ApJ, 449, 105
Leahy, D. A., & Creighton, J. 1993, MNRAS, 263, 314
Levine, A. M., Bradt, H., Cui, W., Jernigan, J. G., Morgan, E. H., Remillard, R., Shirey, R. E., & Smith, D. A. 1996, ApJ, 469, L33
Lightman, A. P., & White, T. R. 1988, ApJ, 335, 57
Magdziarz, P., & Zdziarski, A. A. 1995, MNRAS, 273, 837
Miyazaki, S., et al. 1996, PASJ, 48, 801
Morini, M., Anselmo, F., & Molteni, D. 1989, ApJ, 347, 750
Mushotzky, R. F., Serlemitsos, P. J., Becker, R. H., Boldt, E. A., & Holt, S. S. 1978, ApJ, 220, 790
Nandra, K., et al. 1997, ApJ, 477, 602
Nandra, K., & Pounds, K. A. 1994, MNRAS, 268, 405
Rothschild, R. E., et al. 1998, ApJ, 496, 538
Steinle, H., et al. 1998, A&A, 330, 97
Sugizaki, M., Inoue, H., Sonobe, T., Takahashi, T., & Yamamoto, Y. 1997, PASJ, 49, 59
Turner, T. J., George, I. M., Mushotzky, R. F., & Nandra, K. 1997a, ApJ, 475, 118
Turner, T. J., George, I. M., Nandra, K., & Mushotzky, R. F. 1997b, ApJ, 488, 164
———. 1997c, ApJS, 113, 23
Wang, B., Inoue, H., Koyama, K., Tanaka, Y., Hirano, T., & Nagase, F. 1986, PASJ, 38, 685
Woźniak, P. R., Zdziarski, A. A., Smith, D., Madejski, G. M., & Johnson, W. N. 1998, MNRAS, 299, 449
Zdziarski, A. A., Johnson, W. N., Done, C., Smith, D., & McNaron-Brown, K. 1995, ApJ, 438, L63
Zdziarski, A. A., Johnson, W. N., & Magdziarz, P. 1996, MNRAS, 283, 193